Bioconjugate Chemistry

ARTICLE

pubs.acs.org/bc

Biotin-4-Fluorescein Based Fluorescence Quenching Assay for Determination of Biotin Binding Capacity of Streptavidin Conjugated Quantum Dots

Rowena Mittal[†,§] and Marcel P. Bruchez[*,‡,§]

[†]Department of Biomedical Engineering

[‡]Department of Chemistry

[§]Molecular Biosensor & Imaging Center

Carnegie Mellon University, Pittsburgh, Pennsylvania 15213, United States

Supporting Information

ABSTRACT: The valency of quantum dot nanoparticles conjugated with biomolecules is closely related to their performance in cell tagging, tracking, and imaging experiments. Commercially available streptavidin conjugates (SAv QDs) are the most commonly used tool for preparing QD−biomolecule conjugates. The fluorescence quenching of biotin-4-fluorscein (B4F) provides a straightforward assay to quantify the number of biotin binding sites per SAv QD. The utility of this method was demonstrated by quantitatively characterizing the biotin binding capacity of commercially available amphiphilic poly(acrylic acid) Qdot ITK SAv conjugates and poly(ethylene glycol) modified Qdot PEG SAv conjugates with emission wavelengths of 525, 545, 565, 585, 605, 625, 655, 705, and 800 nm. Results showed that 5- to 30-fold more biotin binding sites are available on ITK SAv QDs compared to PEG SAv QDs of the same color with no systematic variation of biotin binding capacity with size.

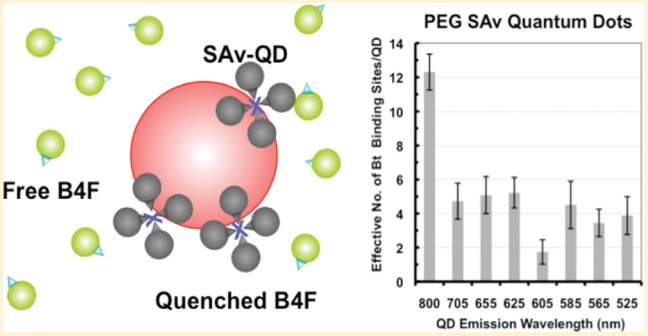

INTRODUCTION

QDs are semiconductor nanoparticles that have size and composition tunable fluorescence emission spectra, narrow emission bands, and very high levels of brightness and photostability.[1−3] In the 12 years since quantum dots (QDs) were first rendered biochemically stable for biological applications,[4,5] many groups have been working to optimize or apply QD conjugates to answer biological, biomedical, and clinical research questions.[5−20] A wide number of approaches have been used to chemically modify QDs with biomolecules and to apply them to a range of assays and imaging methods.[4,5,7,9,12,15,16,21−23] The most practical bioconjugation method to emerge makes use of the high-affinity and selective interaction of biotinylated ligands with commercially available SAv QD conjugates. For example, SAv QDs can be used to perform multicolor analysis of multiple antigen-specific cell populations in flow cytometry. By creating QD conjugates or MHC tetramers targeted toward a variety of cell surface proteins, one can reveal phenotypic characteristics important in understanding cell differentiation and immune responses.[24] Others have used SAv QDs conjugated to biotin-modified proteins of interest to target and image cellular structures such as membrane receptors, actin, nuclear antigens, or DNA.[9,14−16,19,20,25−27]

As colloidal materials, synthesized QD conjugates are known to vary in physiochemical and biochemical properties. This variation has resulted in differences in cellular uptake, subcellular localization, and systemic distribution of QDs bearing different surface characteristics in vivo.[28] Since they are colloidal materials, QDs tend to have multiple biological ligands linked on a single particle. Hence, QDs have biophysical and biological properties that are distinct from typical dye conjugates. For many biophysical and cell biology studies, stoichiometry must be adjusted to avoid multivalency issues such as receptor cross-linking. However, published methods for quantifying bioactivity of QD conjugates are material intensive or rely on special equipment.

Ligand density is known to affect cell internalization of recognized substrates,[29] and variations in QD valency can affect cross-linking of surface proteins, activating signaling pathways and reducing receptor mobility.[18,20,30,31] Such variation in QD bioactivity makes protocols unreliable and questions dependent on the binding capacity of QDs difficult to answer. For example, Wu et al. were unable to use biotin beads to develop flow cytometry calibration standards because the valency of SAv QDs was unregulated, as witnessed by inconsistent flow cytometry readings.[32] In addition, variable valency can affect the quantitation of fluorescent binding experiments.

Received: July 23, 2010
Revised: December 27, 2010
Published: February 11, 2011

Table 1. Summary of Literature Reports of Binding Capacity of SAv QDs[30,32,48,50,53−56]

no. of SAv per QD	no. of biotin binding sites per QD	source
4 to 10	16 to 40	Howarth, 2008
5 to 10	15 to 30	Young, 2005
5 to 10	-	Vu, 2005
5 to 10	-	Lidke, 2007
6 to 8	2 to 3	Invitrogen, 2006
8 to 10	-	Wu, 2007
-	10	Swift, 2006
10	-	Carstairs, 2009
15 to 25	-	Zhang, 2005
-	20	Ruan, 2007

Conjugate valency is an essential parameter to determine for any conjugate, yet there are few reports and even fewer methods published for routine characterization of QD valency. Using an isotope dilution method, Cai et al. quantified the number of RGD peptides per QD particle.[1] Clarke et al. developed a radiolabeling assay to track the attachment of small biomolecules to QD surfaces.[33] Swift et al. determined the number of biotin binding sites per SAv QD using biotinylated QDs in a blocking binding assay with two-photon excitation fluorescence cross-correlation spectroscopy (TPE-XCS) analysis.[34] Additional methods using chromatographic or electrophoretic techniques, gel electrophoresis, and AFM qualitatively address questions of QD size, morphology, and mobility related to valency.[17,18,28,30,35−38] It is essential to quantify the bioactivity of each preparation of QD conjugates, to account for nonuniformities in size, surface chemistry, and coupling efficiency.[39] This is sine qua non for dye conjugates and represents a significant shortcoming in the literature of QD conjugates. The ability to correlate QD valency with bioactivity and performance will allow determination of the optimum number of bioligands required for efficient conjugate preparation or delivery into cells[12,26] and may provide a quantitative basis for variations seen in both commercially available and homemade QDs.

Our group previously developed a method to code mammalian cells with QDs utilizing commercially available SAv QDs and biotinylated polyarginine (polyarg) peptide.[36] In this past work, the half-saturation of polyarg conjugated QD (polyarg QD) uptake by Swiss 3T3 mouse fibroblast cells was reached at 27-fold molar excess of polyarg to SAv QD. While loosely related to valency of the QDs under study, this phenomenological value is dependent on experimental conditions and cell type and not a direct measurement of the nanoparticle valency. Currently, there is no clear or practical method by which researchers can determine a quantitative value for the binding capacity of SAv QDs for biotinylated ligands. Researchers rely on rough estimates of valency based on starting material concentrations in the conjugation reaction, rough estimates based on mobility assays, or rough estimates as provided by the manufacturer. Traditional methods of absorbance ratios or HABA filtrations are of limited utility due to the large UV absorbance cross-section of QDs. The literature reports a wide range of values for either the number of SAv per QD or number of biotin binding sites per QD as shown in Table 1. The goal of this study was to develop a rapid, straightforward, and quantitative method that utilizes minimal QD stock material to directly measure the biotin binding capacities of SAv QDs.

Our approach was to apply a biotin-4-fluorescein (B4F) quenching titration assay to QDs to characterize the number of biotin binding sites per QD. B4F is a commercially available dye, which quenches upon binding to SAv.[40−45] The number of biotin-binding sites is determined by the point of intersection between two binding regimes in a titration of the conjugate with B4F.[40−43,46] The first regime of fluorescence quenching occurs at lower concentrations of B4F ligand relative to conjugate concentration. Here, B4F molecules are quantitatively bound by the available biotin binding sites. There is some nonlinearity in this regime due to the fact that the extent of B4F fluorescence quenching varies with the number of B4F molecules bound per substrate molecule.[40] The most pronounced quenching occurs when all four sites of the SAv are bound with B4F. In a 4-to-1 B4F-to-SAv complex, the extent of B4F fluorescence quenching by SAv is 88%. [40] After the saturation point, a second linear regime of concentration-dependent fluorescence occurs at higher concentrations of B4F ligand to substrate concentration. This fluorescence assay detects down to 0.5 nM binding sites in purified proteins with 30 min incubation conditions. [40] This method provides a direct measurement of available binding sites, rather than the number of conjugated proteins. Where questions of ligand stoichiometry are important, this technique gives a more accurate, quantitative description of biochemical valency compared to size or charge dependent analyses. This method was applied to a range of commercial SAv functionalized QDs.

EXPERIMENTAL PROCEDURES

Calibration of B4F Concentration. The estimated or "nominal" concentration of B4F was determined from measured absorbance of B4F (Invitrogen) at 495 nm obtained by UV−vis spectroscopy on a PerkinElmer Lambda 45 instrument, based on an extinction coefficient of 68 000 M^{-1} cm^{-1}.[40,43,44] Kada et al. note uncertainty associated with this molar extinction coefficient, which can be calibrated for effective concentration of B4F using a known amount of substrate with certain extinction coefficient and number of binding sites.[40,42,46] In this case, we used SAv to calibrate B4F concentration because it is well-known to have 4 biotin binding sites per molecule. [47] The concentration of SAv (Sigma) was determined from measured absorbance of SAv at 280 nm with an extinction coefficient of 204 000 M^{-1} cm^{-1} as provided by the manufacturer.[47] 1 nM SAv was titrated with a 2-fold serial dilution of B4F in terms of nominal concentration as described in the assay below. Since there are 4 binding sites per SAv molecule, the intersection point of the titration marking saturation of all binding sites per SAv should occur at 4 nM B4F. Therefore, the value of the intersection point, in terms of nominal concentration, is divided by 4 to obtain a correction factor for effective concentration. Then, values of biotin binding site per particle, in terms of nominal concentration, are divided by the correction factor to obtain the number of biotin binding sites per particle, in terms of effective concentration.

B4F Fluorescence Binding Assay of SAv and SAv QDs. In black-walled, flat, clear-bottomed 96 well plates (CoStar), 1 nM (QD concentrations as provided by manufacturer) poly(ethylene glycol) (PEG) SAv QDs (Invitrogen) with emission wavelengths (nm) of 525 (Qdot SAv conjugate Q10141MP), 565 (Qdot SAv conjugate Q10131MP), 585 (Qdot SAv conjugate Q10111MP), 605 (Qdot SAv conjugate Q10101MP), 625 (Qdot SAv conjugate A10196), 655 (Qdot SAv conjugate Q10121MP), 705 (Qdot SAv conjugate Q10161MP), and 800 (Qdot SAv conjugate Q10171MP); poly(acrylic acid) amphilic

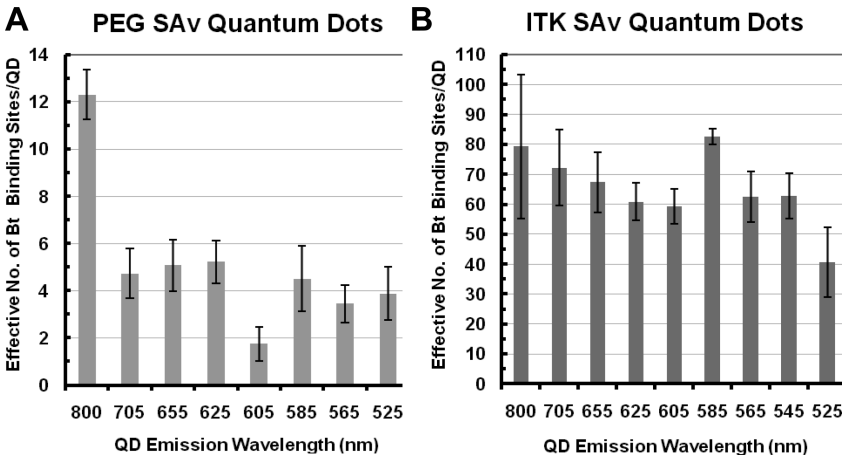

Figure 1. Effective biotin binding capacity per particle by B4F fluorescence quenching assay. (A) PEG SAv QDS, (B) ITK SAv QDs. Error bars represent standard deviation of the mean of independent triplicate samples.

(AMP) SAv QDs (Invitrogen) with emission wavelengths (nm) of 525 (Qdot ITK SAv conjugate Q10041MP), 545 (Qdot ITK SAv conjugate Q10091MP), 565 (Qdot ITK SAv conjugate Q10031MP), 585 (Qdot ITK SAv conjugate Q10011MP), 605 (Qdot ITK SAv conjugate Q10001MP), 625 (Qtracker Cell Labeling Kit: Component A A10198), 655 (Qdot ITK SAv conjugate Q10021MP), 705 (Qdot ITK SAv conjugate Q10061MP), and 800 (Qdot ITK SAv conjugate Q10071MP); and SAv were titrated in triplicate independent series with a 2-fold serial dilution of nominal 500 nM to 0.488 nM and 0 nM B4F in filtered 0.05 M Tris buffered saline (TBS) pH 8.0 (Sigma). This titration is therefore a noncumulative titration of QDs or SAv. A row of the serial dilution of B4F alone was included as a positive signal control. Samples were incubated for one hour at room temperature in the dark. As a control for specificity between SAv and the biotinylated dye, 525 ITK SAv QDs (Qdot ITK SAv conjugate Q10041MP) and SAv were blocked with 10 μM biotin for 30 min and titrated with B4F as described. Carboxyl QDs (Qdot 705 ITK carboxyl Q21361MP) were also titrated under the same conditions as a control for zero biotin binding sites of unfunctionalized QDs. Using a Tecan Safire2 fluorescence plate reader, wells were measured for fluorescence at 525 nm with excitation at 490 nm and gauging gain off of the highest 525 nm fluorescence signal: 500 nM biotin-4-fluorescein without QDs or SAv.

Filtration of B4F Dye. PEG and ITK SAv 525 and 705 QDs, SAv, and B4F alone were assayed as described above. Afterward, samples were transferred to 10 000 or 30 000 MW cutoff filter plates (Millipore or Pall, respectively) and centrifuged at 3000 *g* for 1 h or 10 min, respectively. Eluent was transferred to optical well plates and analyzed using a Tecan Safire2 fluorescence plate reader for fluorescence at 525 nm with excitation at 490 nm and gauging gain off of the highest 525 nm fluorescence signal: 500 nM biotin-4-fluorescein without QDs or SAv.

Data and Statistical Analysis. Background fluorescence signal at 0 nM B4F for SAv and SAv QDs was subtracted from signal at 500 nM to 0.488 nM B4F. The signal for each species was plotted against B4F nominal concentration. Using *GraphPad Prism* software, the linear regime of each series was defined by the points that fell on a linear regression by robust R^2 value (closest to 1.0) and inspection. Since fluorescence is linear with dye concentration, we can be certain about the points that fit a linear regression. The first outlier of the linear regression was used to define the end of the nonlinear regime. The nonlinear regime was fit to a second-order polynomial; the nonlinearity is the result of stronger fluorescence quenching of B4F when 3−4 versus 1−2 biotin binding sites per SAv molecule are occupied.[40,43] The intersection point of the titration was determined by solving for the positive root of the polynomial generated from the equivalence of the two-fit function using *Matlab* software. The *x*-value of the root represents the number of biotin sites per particle. Standard deviations of the roots of the polynomial were calculated using *Matlab* from the standard deviation of the coefficients of the polynomial and linear fits. The numbers of biotin binding sites were converted from terms of nominal concentration to terms of effective concentration of B4F by dividing by the correction factor obtained in the calibration of B4F concentration with SAv as described in *Calibration of B4F Concentration*. While graphical analysis was conducted in linear scale, titration profiles were plotted in log−log scale for presentation.

Table 2. Number of Biotin Binding Sites per SAv QD

	number of biotin binding sites			
	PEG SAv QDs		ITK SAv QDs	
emission wavelength (nm)	value (SD)	cat no	value (SD)	cat no
525	4 (1)	Q10141MP	41 (12)	Q10041MP
545	NA	NA	63 (8)	Q10091MP
565	3 (1)	Q10131MP	62 (8)	Q10031MP
585	5 (1)	Q10111MP	83 (16)	Q10011MP
605	2 (1)	Q10101MP	60 (7)	Q10001MP
625	5 (1)	A10196	61 (6)	A10198
655	5 (1)	Q10121MP	67 (10)	Q10021MP
705	5 (1)	Q10161MP	72 (13)	Q10061MP
800	12 (1)	Q10171MP	79 (24)	Q10071MP

RESULTS

The approach described in this paper is a quick, simple assay relying on small volumes of stock QD material (4−10 μL given stock at 1−2 μM) that can be used routinely to characterize the

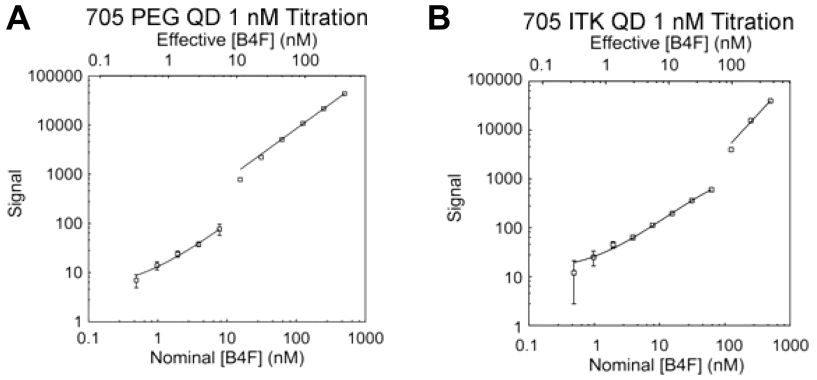

Figure 2. Representative titration profiles of 1 nM PEG SAv and ITK SAv 705 QDs with B4F. (A) Log−log plot of 1 nM PEG SAv 705 QD (Qdot SAv conjugate Q10161MP) titrated with B4F. (B) Log−log plot of 1 nM ITK SAv 705 QD (Qdot ITK SAv conjugate Q10061MP) titrated with B4F. Both titrations resulted in two regimes of fluorescence behavior: the first regime at low concentrations of B4F fit to a second-order polynomial and the second regime at high concentrations of B4F fit to a linear regression. Error bars represent the standard deviation of the mean of independent triplicate series.

number of biotin binding sites on QDs. This fluorescence-quenching assay revealed significant quantitative differences in biotin binding capacity of commercially available SAv QDs (Invitrogen, Corp, Carlsbad, CA). The average number of biotin binding sites per batch of PEG SAv QDs and ITK SAv QDs studied in this work are illustrated in Figure 1 and listed in Table 2. These analyses were conducted on new QD samples, as supplied by the manufacturer, assuming stock materials are free of impurities or unconjugated SAv. If analyses will be conducted on older samples, then ultrafiltration of QD materials prior to titration with B4F would eliminate any free SAv due to degradation from analysis.

Representative titration profiles of PEG versus ITK SAv 705 QDs are shown in Figure 2. To prove the quantitative and accurate nature of this assay despite potential FRET effects or overlap of emission wavelengths between B4F emission and 525 QDs, samples of PEG and ITK SAv QDs with 525 and 705 nm emission wavelengths were measured before and after ultrafiltration (30 kDa) of unbound B4F dye to determine the number of biotin binding sites per particle as shown in Figure 3.

The nominal concentration of B4F in this study was close to the effective concentration derived by titration of a known concentration of free SAv protein (see Supporting Information Figure S1). It is well-known that free SAv has 4 biotin binding sites per molecule.[47] As a result, the factor by which all QD species' nominal binding capacity values were divided by in this work was 1.384.

Unconjugated QDs (Supporting Information Figure S2) and biotin blocked QDs (Supporting Information Figure S3) showed no signature of binding or nonlinearity, thus lacking any measurable biotin binding capacity, and confirming the specificity of the quenching for the biotin−SAv interaction.

Kada et al. have shown that this assay is accurate and reproducible down to 0.5 nM SAv with 30 min incubation.[40] Nevertheless, an incubation time study was conducted which confirmed that this assay was accurate at 1 nM SAv with 1 h incubation (Supporting Information Figure S4) and reproducible (compare to Supporting Information Figure S4 to Figure S1).

DISCUSSION

The biotin binding sites per QD determined by the B4F method as shown in Table 2 are more instructive than the rough estimates reported by the literature and commercial sources as

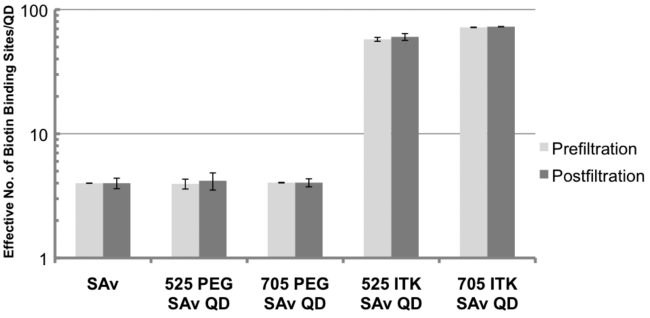

Figure 3. Number of biotin binding sites per particle before and after filter separation of free B4F from particles. Error bars represent standard deviation of the mean of independent triplicate samples.

listed in Table 1. Invitrogen notes that any values they provide are indeed only estimates, dependent on batch, emission wavelength, and steric hindrance of bound SAv.[48] However, assuming estimates of SAv QD valency has been insufficient for a number of research applications.[34,39,49,50] It should be noted that the biotin binding values determined here represent the number of biotin binding sites available to B4F and other molecules with similar steric hindrance characteristics. Therefore, these values may not translate to the number of biotin binding sites available to larger biotinylated molecules. Nonetheless, our method allows for a standard approach for batch-specific characterization of the number of biotin binding sites per QD.

It is clear from Table 2 that there are significantly more biotin binding sites available on ITK SAv QDs compared to PEG SAv QDs. PEG SAv QDs (the regular Qdot SAv conjugates from Invitrogen) utilize a PEG linker chemistry to ensure high-quality staining and low background levels under physiological conditions, whereas ITK SAv QDs have SAv covalently attached to the inner amphiphilic coating without the PEG linker for applications such as fluorescence resonance energy transfer (FRET).[51] Clearly, the PEG linker chemistry results in a significantly lower average number of biotin binding sites. Therefore, it is important to understand which type of SAv QD—PEG modified or unmodified—one has purchased when biotin binding capacity plays a large role in results, as it would in many QD functionalization and labeling experiments.

Figure 3 shows that emission of 525 QDs does not interfere with the accuracy of the B4F titration signal. Notably, B4F fluorescence properties for the purpose of this assay in ITK SAv QDs—where the PEG linker chemistry is omitted—are not affected by FRET effects due to proximity with QDs. Since results were altered by neither filtration nor the removal of QD-bound B4F, there is no interference from the QD absorbance or emission in these results. Filtration is therefore unnecessary, and this assay can be done as a simple "mix-and-read" fluorescence titration.

Invitrogen estimates that QDs of greater size, a characteristic dependent on core composition and emission wavelength, will have a higher number of SAv ligands.[48] However, our results show that this mnemonic is neither consistently nor anecdotally true in an array of commercial samples. Some intermediate-sized QDs, such as the 605-nm-emitting PEG SAv QD and the 585-nm-emitting ITK SAv QD samples, exhibited significantly lower or higher binding capacity compared to larger or smaller QDs as shown in Figure 1 and Table 2. These results underscore the need for a batch-specific characterization method such as the one developed here.

The fluorescence-binding assay described here enables parallel analysis of many samples at one time with minimal sample consumption. According to Invitrogen, the most accurate method for general detection of extent of functionalization on QDs is by size exclusion chromatography, where more highly conjugated QDs would have a longer retention time than less conjugated QDs.[48] Our lab, as well as other laboratories, previously reported using gel electrophoresis to determine the extent of conjugation of a given batch of QD conjugates.[17,18,28,30,35−38,52] However, these methods are material and time intensive and infer conjugation from size rather than directly measuring bioactivity. Lastly, the multiplate assay format requires smaller sample volumes, consuming <4% of the commercially provided material for a triplicate analysis of the biotin binding capacity.

The B4F titration method described and applied in this paper has demonstrated significant variance in biotin binding capacity of commercial QDs of different surface chemistry and emission color. Quantitative characterization of the binding capacity of commercially available amphiphilic polymer stabilized SAv QDs (Qdot ITK SAv conjugate) and poly(ethylene glycol) functional SAv QDs (Qdot SAv conjugate) with emission wavelengths of 525, 545, 565, 585, 605, 625, 655, 705, and 800 nm demonstrated that significantly more biotin binding sites are available on ITK SAv QDs compared to PEG SAv QDs. The number of biotin binding sites per SAv QD does not necessarily increase with QD size across a series of QD colors. Importantly, this assay gives quantitative and accurate information without interference from FRET effects or fluorescence emission overlap with B4F. Measurements using this method give accurate values of SAv QD biotin binding capacity and could be used as a tool to benchmark shelf stability and functionalization chemistry of QD SAv conjugates. This information and the reported methodology should be standard practice for characterization of QD SAv conjugates prior to further conjugation.

■ ASSOCIATED CONTENT

Supporting Information. Figures S1−S4 provide representative curves of B4F concentration calibration, control titrations, and incubation time comparisons for the B4F effective concentration determination. This material is available free of charge via the Internet at http://pubs.acs.org.

■ AUTHOR INFORMATION

Corresponding Author

*Corresponding author. E-mail: bruchez@cmu.edu. Mail: 4400 Fifth Avenue, Pittsburgh, PA 15213. Phone: 412.268.9661. Fax: 412.268.6571.

■ ACKNOWLEDGMENT

R.M. was supported by a Dowd-ICES Fellowship. M.P.B. is supported by the NIH National Technology Centers for Networks and Pathways (TCNP) U54-RR022241. This work was initially supported by the NIH Bioengineering Research Partnership (BRP) program (5R01-EB000364). We acknowledge Eric Tulsky and Kari Haley at Invitrogen Corp. for QD samples and Professor Phil Campbell for useful discussions.

■ NOMENCLATURE

B4F Biotin-4-fluorescein
SAv QD Streptavidin quantum dot conjugate

■ REFERENCES

(1) Cai, W. B., Olafsen, T., Zhang, X. Z., Cao, Q. Z., Gambhir, S. S., Williams, L. E., Wu, A. M., and Chen, X. Y. (2007) PET imaging of colorectal cancer in xenograft-bearing mice by use of an F-18-labeled T84.66 anti-carcinoembryonic antigen diabody. *J. Nucl. Med. 48*, 304–310.

(2) Chan, W. C. W., Maxwell, D. J., Gao, X. H., Bailey, R. E., Han, M. Y., and Nie, S. M. (2002) Luminescent quantum dots for multiplexed biological detection and imaging. *Curr. Opin. Biotechnol. 13*, 40–46.

(3) Watson, A., Wu, X. Y., Bruchez, M. (2003) Lighting up cells with quantum dots. *Biotechniques 34*, 296−300, 302−3.

(4) Bruchez, M., Moronne, M., Gin, P., Weiss, S., and Alivisatos, A. P. (1998) Semiconductor nanocrystals as fluorescent biological labels. *Science 281*, 2013–2016.

(5) Chan, W. C. W., and Nie, S. M. (1998) Quantum dot bioconjugates for ultrasensitive nonisotopic detection. *Science 281*, 2016–2018.

(6) Akerman, M. E., Chan, W. C. W., Laakkonen, P., Bhatia, S. N., and Ruoslahti, E. (2002) Nanocrystal targeting in vivo. *Proc. Natl. Acad. Sci. U.S.A. 99*, 12617–12621.

(7) Dubertret, B., Skourides, P., Norris, D. J., Noireaux, V., Brivanlou, A. H., and Libchaber, A. (2002) In vivo imaging of quantum dots encapsulated in phospholipid micelles. *Science 298*, 1759–1762.

(8) Hanaki, K., Momo, A., Oku, T., Komoto, A., Maenosono, S., Yamaguchi, Y., and Yamamoto, K. (2003) Semiconductor quantum dot/albumin complex is a long-life and highly photostable endosome marker. *Biochem. Biophys. Res. Commun. 302*, 496–501.

(9) Jaiswal, J. K., Mattoussi, H., Mauro, J. M., and Simon, S. M. (2003) Long-term multiple color imaging of live cells using quantum dot bioconjugates. *Nat. Biotechnol. 21*, 47–51.

(10) Jamieson, T., Bakhshi, R., Petrova, D., Pocock, R., Imani, M., and Seifalian, A. M. (2007) Biological applications of quantum dots. *Biomaterials 28*, 4717–4732.

(11) Larson, D. R., Zipfel, W. R., Williams, R. M., Clark, S. W., Bruchez, M. P., Wise, F. W., and Webb, W. W. (2003) Water-soluble quantum dots for multiphoton fluorescence imaging in vivo. *Science 300*, 1434–1436.

(12) Mattheakis, L. C., Dias, J. M., Choi, Y. J., Gong, J., Bruchez, M. P., Liu, J. Q., and Wang, E. (2004) Optical coding of mammalian cells using semiconductor quantum dots. *Anal. Biochem. 327*, 200–208.

(13) Medintz, I. L., Uyeda, H. T., Goldman, E. R., and Mattoussi, H. (2005) Quantum dot bioconjugates for imaging, labelling and sensing. *Nat. Mater. 4*, 435–446.

(14) Michalet, X., Pinaud, F. F., Bentolila, L. A., Tsay, J. M., Doose, S., Li, J. J., Sundaresan, G., Wu, A. M., Gambhir, S. S., and Weiss, S. (2005) Quantum dots for live cells, in vivo imaging, and diagnostics. *Science 307*, 538–544.

(15) Rosenthal, S. J., Tomlinson, A., Adkins, E. M., Schroeter, S., Adams, S., Swafford, L., McBride, J., Wang, Y. Q., DeFelice, L. J., and Blakely, R. D. (2002) Targeting cell surface receptors with ligand-conjugated nanocrystals. *J. Am. Chem. Soc. 124*, 4586–4594.

(16) Wu, X. Y., Liu, H. J., Liu, J. Q., Haley, K. N., Treadway, J. A., Larson, J. P., Ge, N. F., Peale, F., and Bruchez, M. P. (2003) Immunofluorescent labeling of cancer marker Her2 and other cellular targets with semiconductor quantum dots (vol 21, pg 41, 2003). *Nat. Biotechnol. 21*, 452–452.

(17) Sperling, R. A., Pellegrino, T., Li, J. K., Chang, W. H., and Parak, W. J. (2006) Electrophoretic separation of nanoparticles with a discrete number of functional groups. *Adv. Funct. Mater. 16*, 943–948.

(18) Nehilla, B. J., Vu, T. Q., and Desai, T. A. (2005) Stoichiometry-dependent formation of quantum dot-antibody bioconjugates: A complementary atomic force microscopy and agarose gel electrophoresis study. *J. Phys. Chem. B 109*, 20724–20730.

(19) Dahan, M., Levi, S., Luccardini, C., Rostaing, P., Riveau, B., and Triller, A. (2003) Diffusion dynamics of glycine receptors revealed by single-quantum dot tracking. *Science 302*, 442–445.

(20) Pinaud, F., King, D., Moore, H. P., and Weiss, S. (2004) Bioactivation and cell targeting of semiconductor CdSe/ZnS nanocrystals with phytochelatin-related peptides. *J. Am. Chem. Soc. 126*, 6115–6123.

(21) Gerion, D., Parak, W. J., Williams, S. C., Zanchet, D., Micheel, C. M., and Alivisatos, A. P. (2002) Sorting fluorescent nanocrystals with DNA. *J. Am. Chem. Soc. 124*, 7070–7074.

(22) Goldman, E. R., Balighian, E. D., Mattoussi, H., Kuno, M. K., Mauro, J. M., Tran, P. T., and Anderson, G. P. (2002) Avidin: A natural bridge for quantum dot-antibody conjugates. *J. Am. Chem. Soc. 124*, 6378–6382.

(23) Pathak, S., Choi, S. K., Arnheim, N., and Thompson, M. E. (2001) Hydroxylated quantum dots as luminescent probes for in situ hybridization. *J. Am. Chem. Soc. 123*, 4103–4104.

(24) Chattopadhyay, P. K., Price, D. A., Harper, T. F., Betts, M. R., Yu, J., Gostick, E., Perfetto, S. P., Goepfert, P., Koup, R. A., De Rosa, S. C., Bruchez, M. P., and Roederer, M. (2006) Quantum dot semiconductor nanocrystals for immunophenotyping by polychromatic flow cytometry. *Nat. Med. 12*, 972–977.

(25) Mansson, A., Sundberg, M., Balaz, M., Bunk, R., Nicholls, I. A., Omling, P., Tagerud, S., and Montelius, L. (2004) In vitro sliding of actin filaments labelled with single quantum dots. *Biochem. Biophys. Res. Commun. 314*, 529–534.

(26) Lidke, D. S., Nagy, P., Heintzmann, R., Arndt-Jovin, D. J., Post, J. N., Grecco, H. E., Jares-Erijman, E. A., and Jovin, T. M. (2004) Quantum dot ligands provide new insights into erbB/HER receptor-mediated signal transduction. *Nat. Biotechnol. 22*, 198–203.

(27) Derfus, A. M., Chan, W. C. W., and Bhatia, S. N. (2004) Probing the cytotoxicity of semiconductor quantum dots. *Nano Lett. 4*, 11–18.

(28) Ballou, B., Lagerholm, B. C., Ernst, L. A., Bruchez, M. P., and Waggoner, A. S. (2004) Noninvasive imaging of quantum dots in mice. *Bioconjugate Chem. 15*, 79–86.

(29) Cai, W. B., Shin, D. W., Chen, K., Gheysens, O., Cao, Q. Z., Wang, S. X., Gambhir, S. S., and Chen, X. Y. (2006) Peptide-labeled near-infrared quantum dots for imaging tumor vasculature in living subjects. *Nano Lett. 6*, 669–676.

(30) Howarth, M., Liu, W. H., Puthenveetil, S., Zheng, Y., Marshall, L. F., Schmidt, M. M., Wittrup, K. D., Bawendi, M. G., and Ting, A. Y. (2008) Monovalent, reduced-size quantum dots for imaging receptors on living cells. *Nat. Methods 5*, 397–399.

(31) Saxton, M. J., and Jacobson, K. (1997) Single-particle tracking: Applications to membrane dynamics. *Annu. Rev. Biophys. Biomol. Struct. 26*, 373–399.

(32) Wu, Y., Campos, S. K., Lopez, G. P., Ozbun, M. A., Sklar, L. A., and Buranda, T. (2007) The development of quantum dot calibration beads and quantitative multicolor bioassays in flow cytometry and microscopy. *Anal. Biochem. 364*, 180–192.

(33) Clarke, S. J., Hollmann, C. A., Aldaye, F. A., and Nadeau, J. L. (2008) Effect of ligand density on the spectral, physical, and biological characteristics of CdSe/ZnS quantum dots. *Bioconjugate Chem. 19*, 562–568.

(34) Swift, J. L., Heuff, R., and Cramb, D. T. (2006) A two-photon excitation fluorescence cross-correlation assay for a model ligand-receptor binding system using quantum dots. *Biophys. J. 90*, 1396–1410.

(35) Carstairs, H. M. J., Lymperopoulos, K., Kapanidis, A. N., Bath, J., and Turberfield, A. J. (2009) DNA Monofunctionalization of quantum dots. *ChemBioChem 10*, 1781–1783.

(36) Lagerholm, B. C., Wang, M. M., Ernst, L. A., Ly, D. H., Liu, H. J., Bruchez, M. P., and Waggoner, A. S. (2004) Multicolor coding of cells with cationic peptide coated quantum dots. *Nano Lett. 4*, 2019–2022.

(37) Parak, W. J., Gerion, D., Zanchet, D., Woerz, A. S., Pellegrino, T., Micheel, C., Williams, S. C., Seitz, M., Bruehl, R. E., Bryant, Z., Bustamante, C., Bertozzi, C. R., and Alivisatos, A. P. (2002) Conjugation of DNA to silanized colloidal semiconductor nanocrystalline quantum dots. *Chem. Mater. 14*, 2113–2119.

(38) Byers, R. J., Di Vizio, D., O'Connell, F., Tholouli, E., Levenson, R. M., Gossard, K., Twomey, D., Yang, Y., Benedettini, E., Rose, J., Ligon, K. L., Finn, S. P., Golub, T. R., and Loda, M. (2007) Semiautomated multiplexed quantum dot-based in situ hybridization and spectral deconvolution. *J. Mol. Diagn. 9*, 20–29.

(39) Hardman, R. (2006) A toxicologic review of quantum dots: Toxicity depends on physicochemical and environmental factors. *Environ. Health Persp. 114*, 165–172.

(40) Kada, G., Falk, H., and Gruber, H. J. (1999) Accurate measurement of avidin and streptavidin in crude biofluids with a new, optimized biotin-fluorescein conjugate. *Biochim. Biophys. Acta 1427*, 33–43.

(41) Kada, G., Kaiser, K., Falk, H., and Gruber, H. J. (1999) Rapid estimation of avidin and streptavidin by fluorescence quenching or fluorescence polarization. *Biochim. Biophys. Acta 1427*, 44–48.

(42) Gruber, H. J., Kada, G., Marek, M., and Kaiser, K. (1998) Accurate titration of avidin and streptavidin with biotin-fluorophore conjugates in complex, colored biofluids. *Biochim. Biophys. Acta 1381*, 203–212.

(43) Ebner, A., Marek, M., Kaiser, K., Kada, G., Hahn, C. D., Lackner, B., and Gruber, H. J. (2008) Application of biotin-4-fluorescein in homogeneous fluorescence assays for avidin, streptavidin, and biotin or biotin derivatives. *Methods Mol. Biol. 418*, 73–88.

(44) Balthasar, S., Michaelis, K., Dinauer, N., von Briesen, H., Kreuter, J., and Langer, K. (2005) Preparation and characterisation of antibody modified gelatin nanoparticles as drug carrier system for uptake in lymphocytes. *Biomaterials 26*, 2723–2732.

(45) Schiestel, T., Brunner, H., and Tovar, G. E. (2004) Controlled surface functionalization of silica nanospheres by covalent conjugation reactions and preparation of high density streptavidin nanoparticles. *J. Nanosci. Nanotechnol. 4*, 504–11.

(46) Waner, M. J., and Mascotti, D. P. (2008) A simple spectrophotometric streptavidin-biotin binding assay utilizing biotin-4-fluorescein. *J. Biochem. Biophys. Methods 70*, 873–877.

(47) *Product information sheet for STREPTAVIDIN from Streptomyces avidinii*, product number S4762, CAS NO.: 9013−20−1, Sigma-Aldrich, Inc., Saint Louis, MO.

(48) Abid, A. (2006) Invitrogen.

(49) Chong, E. Z., Matthews, D. R., Summers, H. D., Njoh, K. L., Errington, R. J., and Smith, P. J. (2007) Development of FRET-based assays in the far-red using CdTe quantum dots. *J. Biomed. Biotechnol. 2007*, 54169.

(50) Zhang, C. Y., Yeh, H. C., Kuroki, M. T., and Wang, T. H. (2005) Single-quantum-dot-based DNA nanosensor. *Nat. Mater. 4*, 826–831.

(51) *Molecular Probes: The Handbook—A Guide to Fluorescent Probes and Labeling Technologies*, Invitrogen, Carlsbad, CA (2010).

(52) Chakraborty, S. K., Fitzpatrick, J. A. J., Phillippi, J. A., Andreko, S., Waggoner, A. S., Bruchez, M. P., and Ballou, B. (2007) Cholera toxin B conjugated quantum dots for live cell Labeling. *Nano Lett. 7*, 2618–2626.

(53) Lidke, D. S., Nagy, P., Jovin, T. M., and Arndt-Jovin, D. J. (2007) Biotin-ligand complexes with streptavidin quantum dots for in vivo cell labeling of membrane receptors. *Methods Mol. Biol. 374*, 69–79.

(54) Ruan, G., Agrawal, A., Marcus, A. I., and Nie, S. (2007) Imaging and tracking of tat peptide-conjugated quantum dots in living cells: new insights into nanoparticle uptake, intracellular transport, and vesicle shedding. *J. Am. Chem. Soc. 129*, 14759–14766.

(55) Vu, T. Q., Maddipati, R., Blute, T. A., Nehilla, B. J., Nusblat, L., and Desai, T. A. (2005) Peptide-conjugated quantum dots activate neuronal receptors and initiate downstream signaling of neurite growth. *Nano Lett. 5*, 603–607.

(56) Young, S. H., and Rozengurt, E. (2006) Qdot nanocrystal conjugates conjugated to bombesin or ANG II label the cognate G protein-coupled receptor in living cells. *Am. J. Physiol. Cell Physiol. 290*, C728–C732.